Tuning the ambipolar behaviour of organic field effect transistors via band engineering

P. R. Warren (ID), J. F. M. Hardigree (ID), A. E. Lauritzen (ID), J. Nelson, and M. Riede (ID)

View Online   Export Citation   CrossMark

ARTICLES YOU MAY BE INTERESTED IN

AVS Quantum Science
Co-published with AIP Publishing
Coming Soon!

Tuning the ambipolar behaviour of organic field effect transistors via band engineering

View Online   Export Citation   CrossMark

P. R. Warren,[1,a] [iD] J. F. M. Hardigree,[1,b] [iD] A. E. Lauritzen,[1] J. Nelson,[2] and M. Riede[1,c] [iD]

AFFILIATIONS

[1] Clarendon Laboratory, Department of Physics, University of Oxford, Parks Road, Oxford OX1 3PU, UK

[2] Department of Physics, Imperial College London, Blackett Laboratory, Prince Consort Road, London SW7 2AZ, UK

[a] Electronic mail: peregrine.warren@physics.ox.ac.uk
[b] Present address: Agira Photonics, 8 Saint Mary's St. Rm. 611, Boston MA 02215, US
[c] Electronic mail: moritz.riede@physics.ox.ac.uk

ABSTRACT

We report on a method for fabricating balanced hole and electron transport in ambipolar organic field-effect transistors (OFETs) based on the co-evaporation of zinc-phthalocyanine (ZnPc) and its fluorinated derivative (F_8ZnPc). The semiconducting behaviour of the OFET can be tuned continuously from unipolar p-type, with a hole mobility in the range of $(1.7 \pm 0.1) \times 10^{-4}$ cm^2/Vs, to unipolar n-type, with an electron mobility of $(1.0 \pm 0.1) \times 10^{-4}$ cm^2/Vs. Devices of the pristine ZnPc and F_8ZnPc show a current on/off ratio of 10^5. By co-evaporating the p-type ZnPc with the n-type F_8ZnPc, we fabricate ambipolar transistors and complementary-like voltage inverters. For the ambipolar devices, the optimum balance between the hole and electron mobilities is found for the blend of 1:1.5 weight ratio with hole and electron mobilities of $(8.3 \pm 0.2) \times 10^{-7}$ cm^2/Vs and $(5.5 \pm 0.1) \times 10^{-7}$ cm^2/Vs, respectively. Finally we demonstrate application of the ambipolar devices in a complementary-like voltage inverter circuit with the performance comparable to an inverter based on separate ZnPc and F_8ZnPc OFETs.

I. INTRODUCTION

Organic semiconductors are of great interest for use in electronics. They combine semiconducting properties with established processing techniques like vacuum and solution coating, which require only low substrate temperatures allowing for deposition on flexible, large-area substrates. Over the three decades since the first reports of organic field effect transistors (OFETs) based on polymer[1] and small molecules,[2] the field has advanced such that applications now include organic integrated circuits[3] and flexible active matrix displays.[4] The majority of materials considered for use in OFETs display p-type conduction, that is, they form accumulation layers of holes at the semiconductor-dielectric interface upon negative bias at the gate. N-type organic semiconductors that have been reported stable at ambient conditions remain comparatively rare.[5,6] To build fully organic integrated circuits based on complementary logic, that is the typical design using p- and n-type transistors, high performance n-type materials are required. However, ambipolar semiconductors, which allow for both polarities of charge to be induced in an OFET, offer an alternative design known as complementary-like logic.[7] In this scheme, ambipolar OFETs replace both the p- and n-type transistors thus circumventing the advanced patterning techniques necessary to deposit two separate materials, simplifying the fabrication process. The electron and hole mobilities in these ambipolar devices must be balanced in order for the resulting logic gates to have symmetrical outputs.[8]

Phthalocyanines have demonstrated both p-type semiconducting behaviour and n-type behaviour depending on the attached side groups.[9,10] Nénon et al.[11] achieved ambipolar behaviour by fabricating heterojunctions of copper phthalocyanine (CuPc) and its fully-fluorinated derivative F_{16}CuPc. They reported that OFETs based on stacked bi-layers of the different CuPc derivatives gave better performance as compared to a 1:1 blend of the two semiconductors. Recent improvements towards balanced ambipolar transport in OFETs has come from Jiang et al.[12] who proposed a method of molecular crystal engineering to tune zinc phthalocyanine (ZnPc) films from p-type to n-type by replacing the hydrogen on the outer
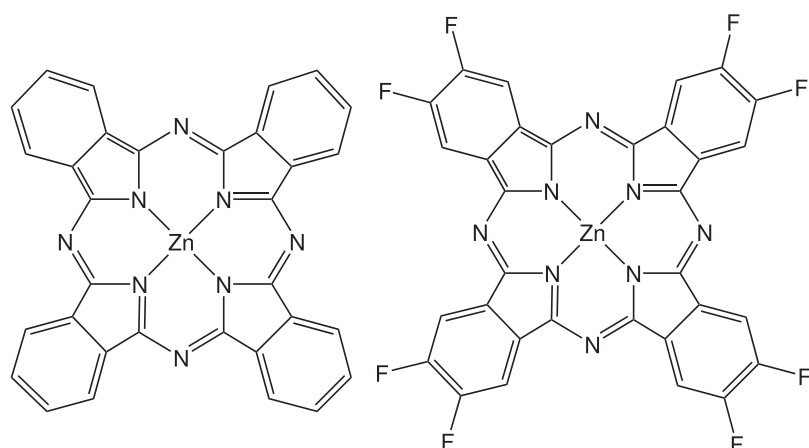
FIG. 1. Molecular structure of zinc phthalocyanine (ZnPc) and its octuply fluorinated derivative (F_8ZnPc).

rings with fluorine F_xZnPc (x = 0, 4, 8, 16). The step-like shift in ionisation potential (IP) by fluorination resulted in a smaller Schottky barrier for electron injection at the organic-gold contacts such that ambipolar behaviour was observed for F_4ZnPc and n-type behaviour for both F_8ZnPc and F_{16}ZnPc.

In this study, we co-evaporate films of ZnPc and F_8ZnPc (chemical structures shown in Figure 1) over a range of blend weight ratios to overcome the limitations of only having discrete energy steps given by the fluorination. This builds on recent work by Schwarze et al.[13] who demonstrated that the IP of a thin film based on the co-deposition of ZnPc with one of its fluorinated derivatives can be linearly tuned as a function of blend ratio. We fabricate and electrically characterise ZnPc:F_8ZnPc OFETs with a range of blend weight ratios from 1:5 to 5:1 which span unipolar p-type to ambipolar to unipolar n-type behaviour. We investigate the morphology of the blended films by GIWAXS measurements and report that the blends appear less ordered than the single component films at the concentrations used for the voltage inverter. Finally we demonstrate the ambipolar OFETs in a complementary-like voltage inverter.

II. EXPERIMENT

Devices were fabricated via thermal evaporation in vacuum using pre-patterned bottom-gate bottom-contact OFET substrates (Fraunhofer IPMS, Germany) consisting of a highly conductive n-doped silicon gate-electrode covered with 230 nm dielectric layer of thermally grown SiO_2. The gold interdigitated source-drain contacts have a thickness of 30 nm, width of 10 mm and a channel length of 10 μm. Prior to vacuum deposition, the substrates were cleaned in an ultrasonic bath for 10 min in 2.5% Hellmanex solution, DI water, acetone and finally ethanol. The substrates were treated with O_2 plasma for 10 min prior to deposition. Films were evaporated at a base pressure of 10^{-6} mbar with a deposition rate between 0.3 to 0.4 Å/s to achieve thicknesses around 21 nm. The samples were transferred to a nitrogen glovebox, without exposure to air, for characterisation.

The electrical characterisation of the OFETs was made using a Keithley 2636B and Keithley 2400 with in-house developed software freely available online.[14] The measurements were carried out

at room temperature, in the dark and under a nitrogen atmosphere. Grazing-incidence wide-angle x-ray scattering (GIWAXS) studies were carried out at the Surface and Interface Diffraction beamline (I07) at the Diamond Light Source (DLS) using a beam energy of 20 keV (0.62 Å) and a Pilatus2M area detector. The samples were probed while inside a vacuum deposition chamber at a pressure of around 10^{-3} mbar with the MINERVA setup as described by Nicklin et al.[15] The sample-to-detector distance was 42.1 cm as determined via AgBeh calibration. Images were converted to 2D reciprocal space using the DAWN software package[16] with an applied solid angle correction. The intensities in the 2D reciprocal space map figures are normalised to the first out-of-plane peak.

III. RESULTS AND DISCUSSION

Figure 2 shows the output and transfer characteristics of OFETs fabricated with ZnPc, F_8ZnPc and a blend of 1:1.5 weight ratio ZnPc to F_8ZnPc. The ZnPc shows unipolar hole transporting behaviour whilst the F_8ZnPc shows unipolar electron transporting behaviour. At low source-drain voltages, V_{ds}, the F_8ZnPc OFET shows a non-linear current increase in its output which indicates that there may be a barrier for electron injection from the gold electrodes to the semiconductor.[17] The current on/off ratio for each of these single-component devices is $\leq 10^5$.

For the blended films we observe conduction of both holes and electrons. With negative gate bias, V_g, holes accumulate at the semiconductor/SiO_2 interface and the device works as a p-type OFET. Whereas for positive V_g, electrons accumulate at the interface and the device operates as an n-type OFET. The output curves for $V_g = 0$ and -10 V show a marked increase of the source-drain current I_{ds} with increasingly negative V_{ds} which is typical of ambipolar devices due to the contribution of drain-induced holes.[11,18] The transfer curve shows a reduced I_{ds} for only a narrow range of V_g, giving an on/off ratio in the range of 10^3.

The field-effect mobilities for the devices as a function of blend ratio are shown in Figure 3. The mobilities were calculated in the saturation regime from the gradient of the straight line fit of $I_{ds}^{1/2}$ vs V_g (the linear regime mobilities follow a similar trend as shown in Figure S1 in the supplementary material). The measured hole
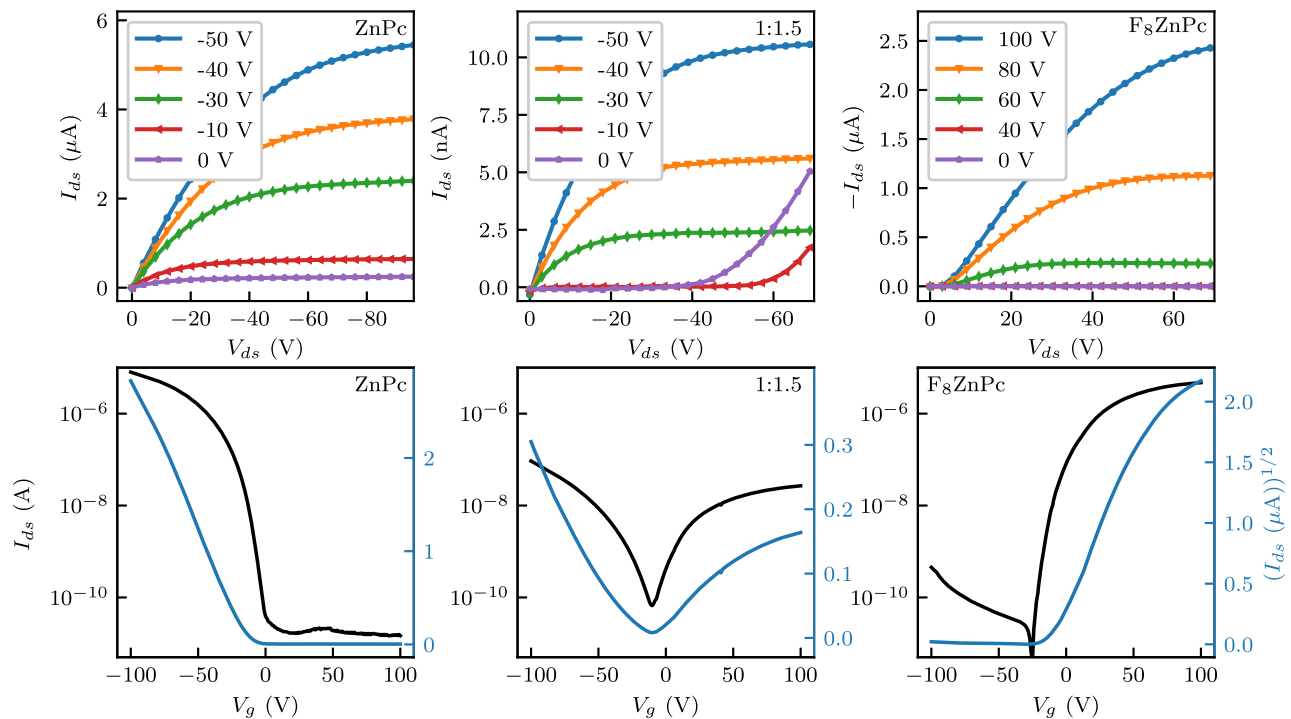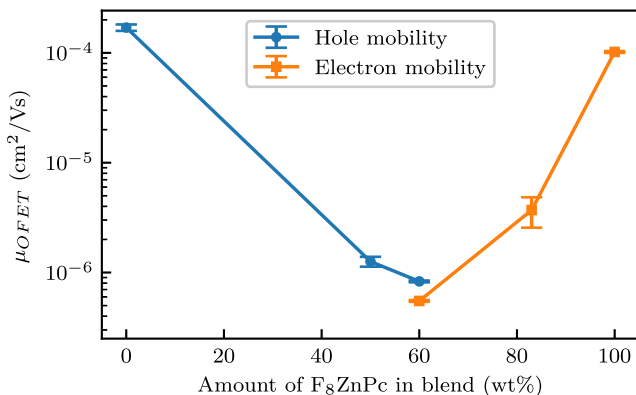
FIG. 2. Output (I_{ds} against V_{ds}) for a range of gate voltages and transfer characteristics (I_{ds} against V_g, with V_{ds} = −50 V) of unipolar pristine ZnPc and F_8ZnPc OFETs alongside a mixed-film ambipolar OFET with weight ratio 1:1.5 ZnPc to F_8ZnPc, all with channel length 10 μm.

mobility for the ZnPc (represented by the 0 % blend in Figure 3) was $(1.7 \pm 0.1) \times 10^{-4}$ cm^2/Vs which is in good agreement with measurements made using a similar geometry in the literature.[19] The electron mobility of F_8ZnPc (100 % blend) was found to be $(1.0 \pm 0.1) \times 10^{-4}$ cm^2/Vs. At a blend ratio of 1:1.5, ambipolar

FIG. 3. Field-effect mobility μ_{OFET} extracted in the OFET saturation regime with channel length of 10 μm. The blend ratio is expressed as a percentage of ZnPc in the blend with 0 % representing ZnPc and 100 % neat F_8ZnPc. The hole mobility is shown as blue circles and the electron mobility is shown as orange squares. Error bars given represent the standard deviation of mobilities measured over four devices from the same deposition run.

behaviour is observed and the hole and electron mobility were found to be $(8.3 \pm 0.2) \times 10^{-7}$ cm^2/Vs and $(5.5 \pm 0.1) \times 10^{-7}$ cm^2/Vs respectively.

This decrease of over two orders of magnitude can be partly attributed to increasing injection barriers for both holes and electrons as the IP and EA of the blended semiconductor shift away from the work function of the gold source-drain electrodes.[20,21] Additionally, these barriers could be embedded in the semiconductor blend itself as well as at the contacts. The distribution of transport states in the blends is expected to be broader than that of the single component films due to the offset between the highest occupied molecular orbitals of the ZnPc and F_8ZnPc.[13] This increases energetic disorder which in turn negatively impacts the mobility.[22] Further disorder may arise through structural inhomogeneities - trap states can localise at grain boundaries resulting in band bending and barriers.[23] This can severely impact charge transport as reported by Bolognesi et al.[24] who observed a drop of three orders of magnitude in field-effect mobility as the grain size in pentacene thin-films decreased.

Grazing Incidence Wide Angle X-ray Scattering (GIWAXS) measurements are carried out to investigate the crystalline structure of the samples. Figures 4a, 4b and 4c show the 2D reciprocal space maps of the ZnPc, 1:1.5 ZnPc:F_8ZnPc weight ratio and F_8ZnPc films. The peaks indicated by arrows in Figure 4a are ascribed to the (200) peak of the herring-bone like α-phase of ZnPc.[11,25] Figures S2a and S2b in the supplementary material show the near out-of-plane and in-plane (at $Q_z = 0.025$ Å^{-1})
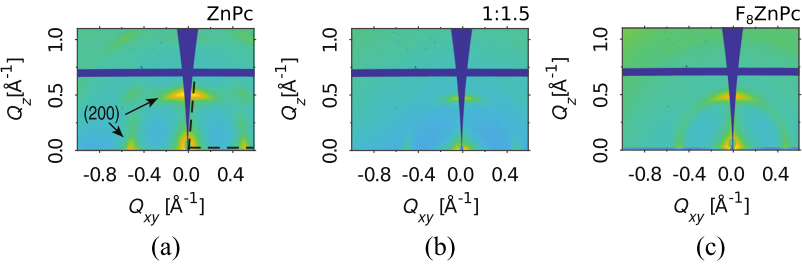
FIG. 4. GIWAXS images of ZnPc, 1:1.5 ZnPc:F$_8$ZnPc weight ratio and F$_8$ZnPc evaporated on SiO$_2$ substrate. For ZnPc, the 200 peaks are indicated. The dashed lines represent the line cuts for d-spacing analysis.

line cuts of the (200) peak of the GIWAXS images as indicated by the dashed lines in Figure 4a.

All films display two preferred orientations indicated by the position of the (200) peak, either fully out-of-plane or fully in-plane. For each configuration, the out-of-plane peak appears more strongly than the in-plane peaks. This indicates that the edge-on orientation is preferred over the face-on configuration.[25] ZnPc (Figure 4a) exhibits greater crystalline ordering than the F$_8$ZnPc as indicated by the visible higher order reflections and strong (200) reflections. Furthermore, the F$_8$ZnPc appears more powder-like suggesting a greater variation of crystallite orientations as compared to the ZnPc. The ZnPc:F$_8$ZnPc blend (Figure 4b) shows the weakest reflection intensities with the in-plane peaks appearing only faintly, indicating less crystalline ordering than in the neat films.

Line cuts were made through the (200) peaks both in-plane and along the near out-of-plane direction to determine the d-spacing of the films. The location of the peaks were fitted with Gaussian functions. The results from the near out-of-plane line cuts, Figure S2a in the supplementary material, are used due to their stronger signal. The location of the peaks and the corresponding d_{200}-spacings are displayed in Table I. The d-spacing of ZnPc is consistent with previously reported values for thermally evaporated thin films.[26] The d-spacing of F$_8$ZnPc is slightly larger than that of ZnPc which is in agreement with trends reported for similar fluorinated phthalocyanines.[11,13] The periodicity of the ZnPc:F$_8$ZnPc blend being closer to the periodicity of the pristine F$_8$ZnPc could indicate that the scattering signal from the blend arises primarily due to ordered F$_8$ZnPc within a host matrix of disordered ZnPc. Alternatively, the ZnPc and F$_8$ZnPc could co-crystallise, with the fluorinated molecules inducing a stacking structure similar to that of pristine F$_8$ZnPc. Reports of intermixing at a molecular level in systems of CuPc:F$_{16}$CuPc are consistent with this latter picture however further work will be needed to verify this co-crystallisation.[11,27]

Finally the OFETs were placed in series, as shown in the inset to Figures 5 and 6, to build voltage inverters, also known as NOT gates.

TABLE I. A table summarising values for the peaks fitted using a Gaussian function from the (200) line cuts shown if Figure S2a in the supplementary material alongside the corresponding d_{200}-spacings.

	Peak (Å^{-1})	d_{200}-spacing (Å)
ZnPc	0.51	12.3
ZnPc:F$_8$ZnPc	0.48	13.1
F$_8$ZnPc	0.49	12.8

Figure 5 shows a voltage inverter based on complementary logic incorporating a pair of p-type (ZnPc) and n-type (F$_8$ZnPc) transistors with a supply voltage V_{dd} = 50V. At voltages below a threshold of around 44V, the p-type OFET is on whilst the n-type OFET is off giving an output voltage almost equal to the supply rail. Above 44V, the p-type OFET switches off and the n-type OFET switches
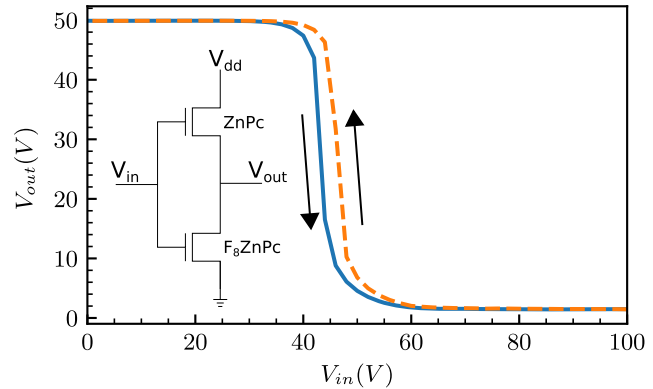

FIG. 5. Transfer characteristics of a complementary inverter with ZnPc in the p-type OFET and F$_8$ZnPc in the n-type OFET. The supply rail was held at V_{dd} = 50 V. The arrows represent the scan direction. The inset diagram shows the circuit configuration.

FIG. 6. Transfer characteristics of an inverter with two ZnPc:F$_8$ZnPc OFETs with weight ratio 1:1.5. The supply rail was held at V_{dd} = 50V. The arrows represent the scan direction. The inset diagram shows the circuit configuration.
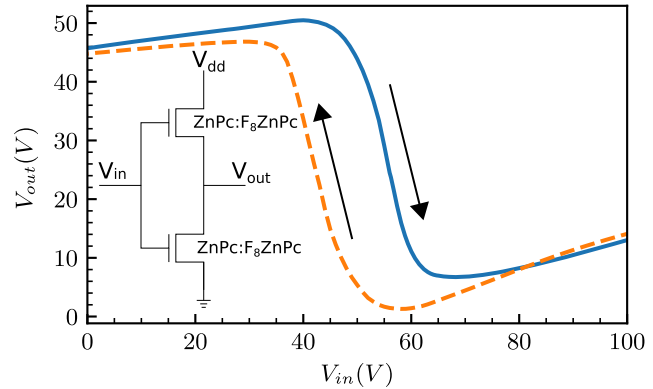
TABLE II. A table summarising the calculated and measured threshold voltages for both the complementary and ambipolar complementary-like (ZnPc:F_8ZnPc) voltage inverters. V_{Tp} and V_{Tn} are the threshold voltages for the p-type and n-type OFETs respectively averaged over four devices scanned in both the forwards and backwards direction. For the complementary-like inverter, V_{Tp} and V_{Tn} are the hole and electron threshold voltages respectively for the 1:1.5 ZnPc:F_8ZnPc OFETs.

	V_{Tp} (V)	V_{Tn} (V)	Calculated V_T (V)	Measured V_T (V)
Complementary inverter	16 ± 11	2 ± 22	38 ± 11	42 ± 2
Ambipolar inverter	25 ± 2	15 ± 4	48 ± 2	50 ± 10

on, resulting in the low state for V_{out}. The threshold voltage (V_T) of an inverter is given by

$$V_T = \frac{(V_{dd} + V_{Tp} + (\mu_n/\mu_p)^{1/2} V_{Tn})}{(1 + (\mu_n/\mu_p)^{1/2})} \qquad (1)$$

where V_{Tp} and V_{Tn} are the threshold voltages for the p-type and n-type OFETs respectively.[28] Taking an average of the threshold voltages over four devices for each material, the calculated threshold voltage of the inverter shown here is (38 ± 11) V which is in agreement with the experimental data (see Table II). The inverter has a gain of 5 with a good noise margin.

As the ambipolar OFETs show both n- and p-type behaviour, complementary-like logic circuits can be realised. Figure 6 shows the transfer characteristics of a voltage inverter driven with $V_{dd} = 50$V composed of two ZnPc:F_8ZnPc OFETs with a blend ratio of 1:1.5. The threshold voltage is calculated as (48 ± 2) V which appears to be in fairly good agreement with the experimental data (Table II). Below the threshold voltage, the output is around 40V and above falls to 10V. The dependence of V_{out} on V_{in} at low and high values of V_{in} can be attributed to the lower on/off ratio in the blended transistors as compared to the pristine ZnPc and F_8ZnPc devices. Consequently there is always a leakage current flowing through the inverter as neither transistor can be fully switched off.[20]

The ambipolar voltage inverter shows a considerable hysteresis as compared to the complementary inverter. This hysteresis is observed when measuring the individual OFETs of the blends at a scan rate of 5 V/s (see Figure S3 in the supplementary material). We have therefore taken averages over forward and backward scans for fitting the mobilities and threshold voltages. Trap related hysteresis has been widely reported in OFETs[29,30] however further time-dependent measurements are necessary here in order to clarify the depth and origin of these traps.

IV. CONCLUSION

In summary, we report a method for fabricating ambipolar OFETs with balanced hole and electron transport based on the co-evaporation of ZnPc and its fluorinated derivative F_8ZnPc. OFETs of the pristine p-type ZnPc show a mobility of $(1.7 \pm 0.1) \times 10^{-4}$ cm^2/Vs measured in the saturation regime. F_8ZnPc OFETs show an electron mobility of a similar magnitude around

$(1.0 \pm 0.1) \times 10^{-4}$ cm^2/Vs. The current on/off ratio of the OFETs in both cases is 10^5. By co-evaporating these two p- and n-type semiconductors, we demonstrate tunable p-type to ambipolar to n-type behaviour dependent on the weight ratio of ZnPc to F_8ZnPc. We find the optimum balance between the hole and electron mobility in the blend of 1:1.5 weight ratio. In this blend, the hole and electron mobility are $(8.3 \pm 0.2) \times 10^{-7}$ cm^2/Vs and $(5.5 \pm 0.1) \times 10^{-7}$ cm^2/Vs for respectively. As these transistors show both p- and n-type behaviour, we fabricate complementary-like voltage inverters which show comparable performance to the inverters based on separate p- and n-type OFETs. The OFET tunability demonstrated here to obtain balanced ambipolar transport could be extended to other systems of organic semiconductors, which permit a shift in their band energies when blended with their halogenated derivatives.

SUPPLEMENTARY MATERIAL

See supplementary material for field-effect mobilities extracted in the linear regime, line cuts from the GIWAXS images and hysteresis curves of the OFETs.

REFERENCES

[1] A. Tsumura, H. Koezuka, and T. Ando, "Macromolecular electronic device: Field-effect transistor with a polythiophene thin film," Applied Physics Letters **49**, 1210–1212 (1986).

[2] G. Horowitz, D. Fichou, X. Peng, Z. Xu, and F. Garnier, "A field-effect transistor based on conjugated alpha-sexithienyl," Solid State Communications **72**, 381–384 (1989).

[3] B. Crone, A. Dodabalapur, Y.-Y. Lin, R. W. Filas, Z. Bao, A. LaDuca, R. Sarpeshkar, H. E. Katz, and W. Li, "Large-scale complementary integrated circuits based on organic transistors," Nature **403**, 521–523 (2000).

[4] L. Zhou, A. Wanga, S. C. Wu, J. Sun, S. Park, and T. N. Jackson, "All-organic active matrix flexible display," Applied Physics Letters **88**, 083502 (2006).

[5] H. E. Katz, A. J. Lovinger, J. Johnson, C. Kloc, T. Siegrist, W. Li, Y. Y. Lin, and A. Dodabalapur, "A soluble and air-stable organic semiconductor with high electron mobility," Nature **404**, 478–481 (2000).

[6] H. Sirringhaus, "Device physics of solution-processed organic field-effect transistors," Advanced Materials **17**, 2411–2425 (2005).

[7] T. D. Anthopoulos, S. Setayesh, E. Smits, M. Cölle, E. Cantatore, B. D. Boer, P. W. M. Blom, and D. M. D. Leeuw, "Air-stable complementary-like circuits based on organic ambipolar transistors," Advanced Materials **18**, 1900–1904 (2006).

[8]M. Bronner, A. Opitz, and W. Brütting, "Ambipolar charge carrier transport in organic semiconductor blends of phthalocyanine and fullerene," Physica Status Solidi (a) **205**, 549–563 (2008).

[9]Z. Bao, A. J. Lovinger, and A. Dodabalapur, "Organic field-effect transistors with high mobility based on copper phthalocyanine," Applied Physics Letters **69**, 3066–3068 (1996).

[10]Z. Bao, A. J. Lovinger, and J. Brown, "New air-stable n -channel organic thin film transistors," **7863**, 207–208 (1998).

[11]S. Nénon, D. Kanehira, N. Yoshimoto, F. Fages, and C. Videlot-Ackermann, "Ambipolar organic field-effect transistors based on CuPc and F16CuPc: Impact of the fine microstructure at organic-organic interface," Synthetic Metals **161**, 1915–1920 (2011).

[12]H. Jiang, P. Hu, J. Ye, Y. Li, H. Li, X. Zhang, R. Li, H. Dong, W. Hu, and C. Kloc, "Molecular crystal engineering: Tuning organic semiconductor from p-type to n-type by adjusting their substitutional symmetry," Advanced Materials **29**, 1605053 (2017).

[13]M. Schwarze, W. Tress, B. Beyer, F. Gao, R. Scholz, C. Poelking, K. Ortstein, A. A. Günther, D. Kasemann, D. Andrienko, and K. Leo, "Band structure engineering in organic semiconductors," Science **352**, 1446–1449 (2016).

[14]P. R. Warren, Keithley-2636, https://github.com/AFMD/keithley-2636 (2018).

[15]C. Nicklin, J. Martinez-Hardigree, A. Warne, S. Green, M. Burt, J. Naylor, A. Dorman, D. Wicks, S. Din, and M. Riede, "MINERVA: A facility to study microstructure and interface evolution in realtime under vacuum," Review of Scientific Instruments **88**, 103901 (2017).

[16]J. Filik, A. W. Ashton, P. C. Y. Chang, P. A. Chater, S. J. Day, M. Drakopoulos, M. W. Gerring, M. L. Hart, O. V. Magdysyuk, S. Michalik, A. Smith, C. C. Tang, N. J. Terrill, M. T. Wharmby, and H. Wilhelm, "Processing two-dimensional X-ray diffraction and small-angle scattering data in *DAWN 2*," Journal of Applied Crystallography **50**, 959–966 (2017).

[17]L. Burgi, T. J. Richards, R. H. Friend, and H. Sirringhaus, "Close look at charge carrier injection in polymer field-effect transistors," J. Appl. Phys. **94**, 6129–6137 (2003).

[18]K. Y. Chung, G. W. Neudeck, and H. F. Bare, "Analytical modeling of the CMOS-like a-Si:H TFT inverter circuit," IEEE Journal of Solid-State Circuits **23**, 566–572 (1988).

[19]S. Pfuetzner, C. Mickel, J. Jankowski, M. Hein, J. Meiss, C. Schuenemann, C. Elschner, A. A. Levin, B. Rellinghaus, K. Leo, and M. Riede, "The influence of substrate heating on morphology and layer growth in C 60: ZnPc bulk heterojunction solar cells," Organic Electronics: Physics, Materials, Applications **12**, 435–441 (2011).

[20]E. J. Meijer, D. M. De Leeuw, S. Setayesh, E. Van Veenendaal, B. H. Huisman, P. W. Blom, J. C. Hummelen, U. Scherf, and T. M. Klapwijk, "Solution-processed ambipolar organic field-effect transistors and inverters," Nature Materials **2**, 678–682 (2003).

[21]A. Bolognesi, A. D. Carlo, and P. Lugli, "Influence of carrier mobility and contact barrier height on the electrical characteristics of organic transistors," Applied Physics Letters **81**, 4646–4648 (2002).

[22]M. Ullah, I. Fishchuck, A. Kadashchuk, P. Stadler, A. Pivrikas, C. Simbrunner, V. N. Poroshin, N. S. Sariciftci, and H. Sitter, "Dependence of Meyer–Neldel energy on energetic disorder in organic field effect transistors," Applied Physics Letters **96**, 213306 (2010).

[23]P. Stallinga, *Electrical characterization of organic electronic materials and devices* (John Wiley & Sons, 2009).

[24]A. Bolognesi, M. Berliocchi, M. Manenti, A. D. Carlo, P. Lugli, K. Lmimouni, and C. Dufour, "Effects of grain boundaries, field-dependent mobility, and interface trap states on the electrical characteristics of pentacene TFT," IEEE Transactions on Electron Devices **51**, 1997–2003 (2004).

[25]J. W. Kim, H. J. Kim, T.-M. Kim, T. G. Kim, J.-H. Lee, J. W. Kim, and J.-J. Kim, "High performance organic planar heterojunction solar cells by controlling the molecular orientation," Current Applied Physics **13**, 7–11 (2013).

[26]S. Senthilarasu, Y. B. Hahn, and S.-H. Lee, "Structural analysis of zinc phthalocyanine (ZnPc) thin films : X-ray diffraction study," Journal of Applied Physics **102**, 043512 (2007).

[27]A. Opitz, B. Ecker, J. Wagner, A. Hinderhofer, F. Schreiber, J. Manara, J. Pflaum, and W. Brütting, "Mixed crystalline films of co-evaporated hydrogen- and fluorine-terminated phthalocyanines and their application in photovoltaic devices," Organic Electronics: Physics, Materials, Applications **10**, 1259–1267 (2009).

[28]Y. Inoue, Y. Sakamoto, Y. Suzuki, M. Kobayashi, Y. Gao, and S. Tokito, "Organic thin-film transistors with high electron mobility based on perfluoropentacene," Japanese Journal of Applied Physics **44**, 3663–3668 (2005).

[29]C. Ucurum, H. Goebel, F. A. Yildirim, W. Bauhofer, and W. Krautschneider, "Hole trap related hysteresis in pentacene field-effect transistors," Journal of Applied Physics **104**, 084501 (2008).

[30]X. Cai, C. P. Gerlach, and C. D. Frisbie, "Current - voltage hysteresis and memory effects in ambipolar organic thin film transistors based on a substituted oligothiophene," J. Phys. Chem. C **111**, 452–456 (2007).